

Title: Integrated Meteorological / Precise Positioning Mission Utilizing Nano-Satellite Constellation

Primary POC: Yuki Sato, Munetaka Kashiwa

Organization: Mitsubishi Electric Corporation Advanced Technology R&D Center

POC email: Sato.Yuki@dn.MitsubishiElectric.co.jp

Need

This mission focuses on the following 2 needs and its objective is to meet both of these needs.

1. The first is in the meteorological field. In order to forecast the occurrence of recent abnormal weather phenomena such as cloudbursts (so-called “guerilla downpours”) and hurricanes and minimize the effect of these phenomena, the local and instantaneous meteorological information is required using low-earth orbit observations.
2. The second is in the precise positioning field. Although technology to factor out GNSS signal errors and perform precise positioning in centimeters accuracy has progressed dramatically, the last remaining issue to realize stable precise positioning unaffected by atmospheric conditions is the tropospheric delay caused by local wet atmospheres. There is a need for technology that accurately estimates this delay.

Mission Objectives

By combining GNSS radio occultation (RO) observations (from edge-on) and thermal infrared observations (from the zenith) using a nano-satellite constellation, local, high precision and high-resolution 3-dimensional distributions of water vapor content and temperature are obtained to fulfill the following objectives:

1. Provide local forecasts to users of the occurrence of abnormal weather phenomena such as cloudbursts (guerilla downpours) and hurricanes.
2. Provide local precise point positioning users with precise information on wet atmosphere tropospheric delay figure information.
3. Increase global forecast accuracy by assimilating data into the meso-scale meteorological model.
4. Increase the estimation accuracy of global GNSS error by assimilating data into the network RTK.
5. Stimulate the development of both meteorological and precise positioning fields in countries and regions that do not possess a meteorological forecast infrastructure or a positioning augmentation infrastructure.

Concept of Operations

The fundamental components are 2 nano-satellites, nano-satellite A that observes the RO of the GNSS from edge-on, and nano-satellite B that acquires thermal infrared images from the zenith. The constellation is composed of multiple A and B. The RO observation data acquired by A is transferred to B through a wireless link. B then downlinks to the RO data received from A and the thermal infrared data taken by B. Ground users will analyze both sets of data to obtain 3-dimensional distribution data of water vapor content and temperature at the observation point (Fig. 1).

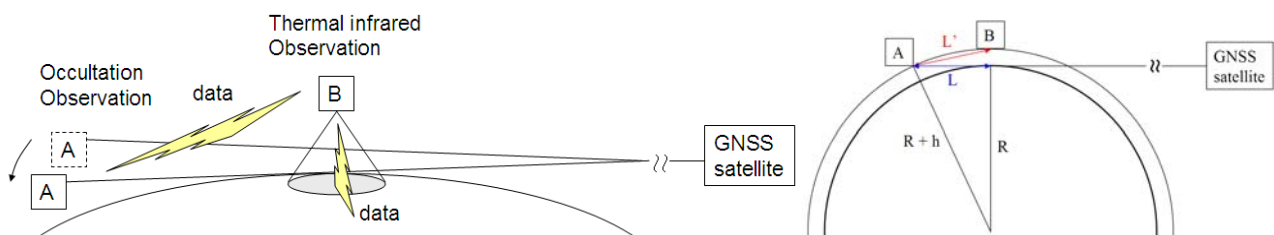


Fig 1 Fundamental Operational Configuration

(1) Notify users when warning signs for cloudbursts (guerilla downpours) and hurricanes can be seen in the 3-dimensional distribution data.

(2) GNSS signal errors that are inherent to GNSS satellites are estimated by existing providers then can be used through concurrent global distribution utilizing infrastructure such as quasi-zenith satellites. Ionospheric delays are eliminated using multi-frequency receivers. Tropospheric delays caused by dry atmospheres are eliminated using high precision models. Tropospheric delays caused by wet atmospheres are calculated and eliminated based on ray analysis [2][3] using 3-dimensional distribution data (Fig. 2).

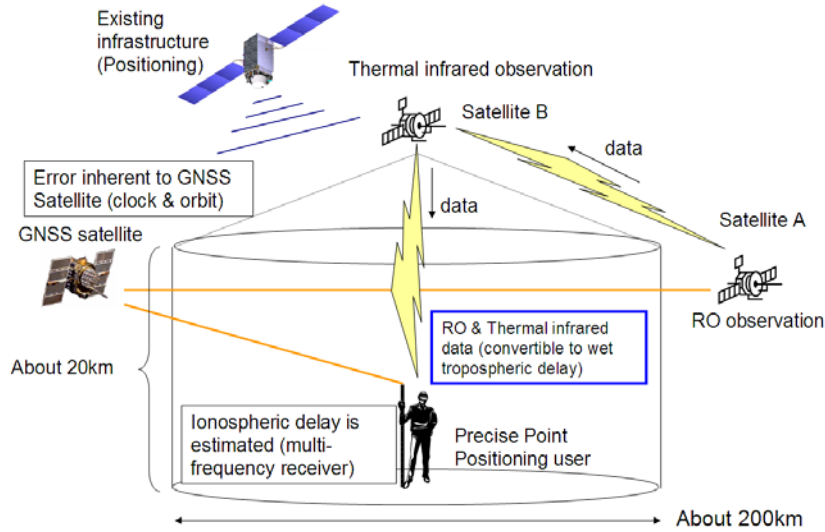


Fig 2 Precise Point Positioning

(3) Improve the forecast accuracy through data assimilation [4] of 3-dimensional distribution data with the meso-scale meteorological model (Fig. 3, left).

(4) Improve the accuracy of generated correction amounts by integrating the 3-dimensional distribution data into the error estimation Kalman filter in the network RTK [5] (Fig.3, right). When atmospheric disturbance levels are especially high, significant improvements in accuracy can be expected when compared to observations using only the ground electric reference point network.

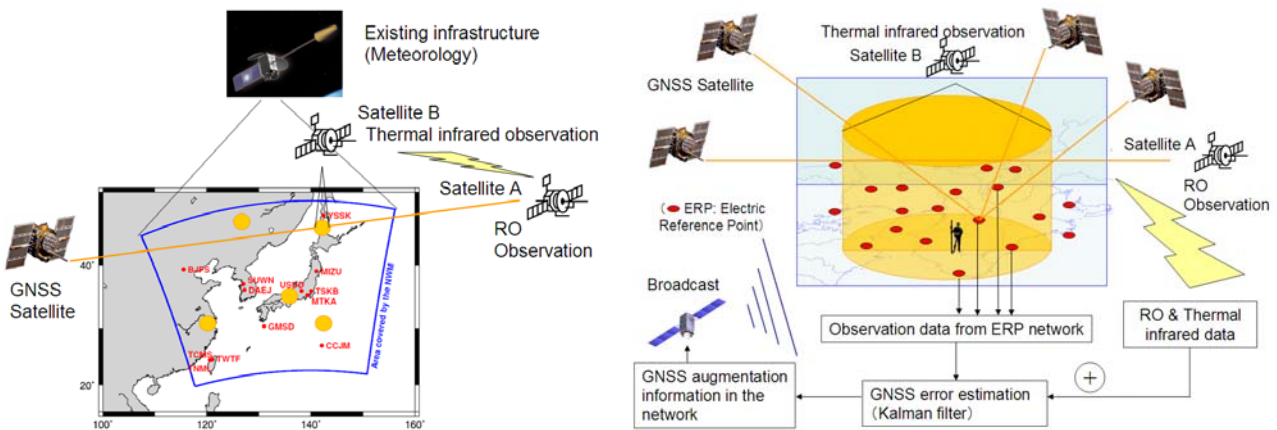


Fig 3 Improving the meso-scale meteorological model (left), improving network RTK accuracy (right)

Key Performance Parameters

1. RO observation resolution (vertical):100m, range: 400m–10km (vertical), 100km (horizontal)
2. Thermal infrared observation resolution (horizontal): 200m, Observation range: 200km in four directions
3. RO receiver sampling frequency: >50Hz, Minimum detectable sensitivity: <20dB-Hz

4. Attitude stability, orbit determination accuracy: $< \pm 3$ deg p-p, < 5 m (Real); < 10 cm rms (Post)
5. Data volume (RO observation, thermal infrared observation): 350k Byte/point (RO 20k Byte + thermal infrared 330k Byte)

Space Segment Description

The external views of Satellite A and satellite B are illustrated in Fig. 4 respectively.

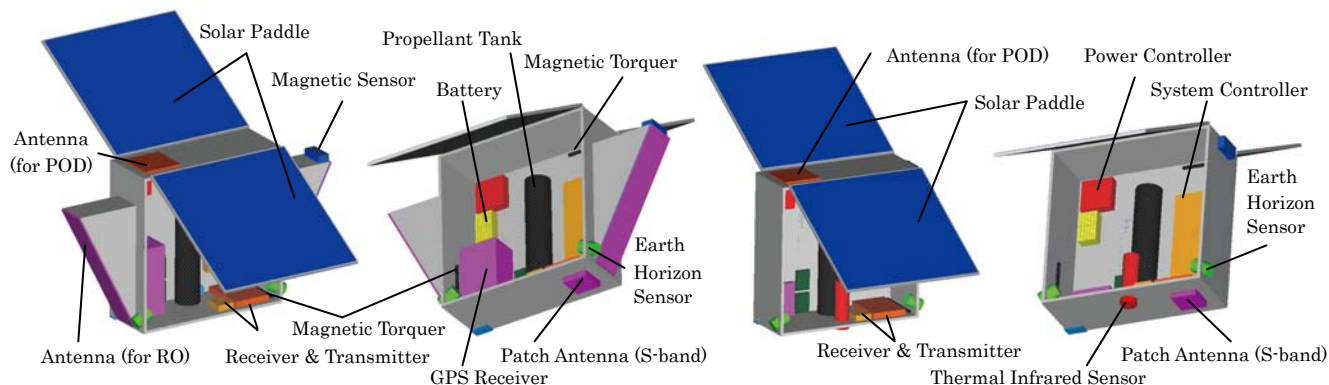


Fig 4 External view of RO observation satellite A (left), thermal infrared observation satellite B (right)

The mass and electrical power of each satellite is as shown below and in Tab 2 (breakdown).

- RO observation satellite A: 15.0 kg, 20 cm×95 cm×50 cm, 29.7 W (average); 42.5W (peak)
- Thermal infrared observation satellite B: 13.8 kg, 20 cm×50 cm×50 cm, 14.2 W (average); 22.5W (peak)

Communications configurations are as shown below. The circuit design charts are as shown in Tab 3.

- Transmission
S band (2.4 GHz band) 1M bps QPSK, UHF band (430 MHz band) 1.2k AFSK / 9.6k bps GMSK
- Receiving
L band (1.2 GHz band) 9.6k bps GMSK, VHF band (144 MHz band) 1.2k AFSK / 9.6k bps GMSK
- Inter-orbit communication: RO data (approximately 150k Byte for 1observation point)
VHF band (144 MHz band) 9.6k bps GMSK

Orbit/Constellation Description

Because the refraction of GNSS radio waves is, at most, approximately 1° , the linear distance L from A to RO observation point P, and linear distance L' to B required to observe P from directly above, is approximately determined by the Earth radius and the satellite altitudes (Fig 1). These are constant values that are not depended on GNSS satellites. Therefore, the key to designing the constellation is “how best to position multiple B satellites along the arc of radius L' in relation to A.”

Here one example of constellation is shown where the orbits of satellites A and B are circular orbits with the same altitude and inclination angle. When the right ascension of ascending nodes (RAAN) are the same and the argument of latitude difference (AOL) is 23.9deg at an altitude of 600km, then $L'=2894$ km can be maintained. This corresponds only for RO observations that occur within the orbital plane of A. Additionally, multiple B are set for several FOV of A by slightly shifting the RAAN and AOL towards A, where the distance of L' is almost maintained.

The result of shifting the RAAN of B to A in 1deg increments from -13deg to 13deg as well as shifting the AOL is as shown (Fig. 7). As shown in the bottom left of Fig. 7, although the lateral distance fluctuates around ± 100 km during one complete orbit, this fluctuation can be absorbed by the 200km coverage of the

thermal infrared sensor. The bottom right of Fig. 7 shows the direction of B in relation to the direction of movement of A for one complete orbit. The directional separation of B is at its widest at the equator and becomes 0 at the north and south poles because of a reversal of direction. The bottom right of Fig. 7 is the range in which RO observation by A and thermal infrared observation of B can occur simultaneously.

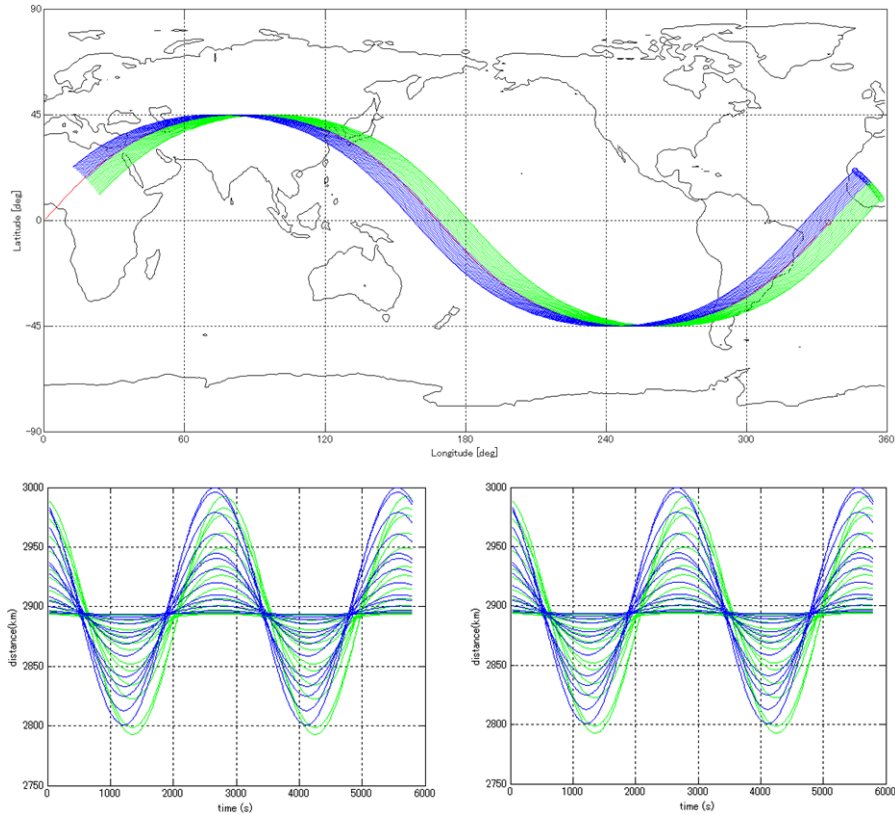


Fig 5 Orbits of A, B (top), distance between A and B (bottom left), angle of B in relation to the direction of movement of A (bottom right): There are 27 B satellites

Implementation Plan

Here implementation plan to realize the constellation of Fig 5 is shown as an example where one satellite A and 27 satellites B are developed. The total life cost is shown in Tab 1. The top level project schedule is described in Fig 6.

Tab 1 The total life cost (less than 6M\$ excluding launch)

| To do | Cost |
|--|---------------------|
| Design & trial manufacture | 1.0M |
| EM development, assembly & testing | 1.0M |
| FM development, assembly & testing (one A & one B) | 1.0M |
| Mass production of B (26 satellites) | 1.56M (=0.06M × 26) |
| Final testing | 1.0M |
| Total | 5.56M |
| Margin | 0.44M |

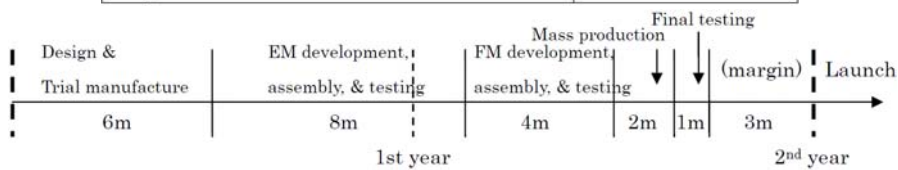


Fig 6 Top level project schedule (less than 2 years before launch)

For existing infrastructure, meteorological satellite (e.g. Himawari) and Positioning satellite (e.g. Michibiki) are involved in this project. The nano-satellite constellation can be supplementary for such service as

provided by these infrastructures. For project risks, failures of separation, failure of constellation deployment are considered. But this project has a strong sustainability because of increasing importance of taking over precise positional information and monitoring local abnormal weather for national security reasons.

Tab 2 Total mass and electrical power

| | Mass [kg] | | | | Power (Ave.) [W] | | | | Power (Peak) [W] | | | |
|---|-----------|----|-----------|--------------|------------------|----|-----------|-------------|------------------|----|-----------|-------------|
| | Mass [kg] | No | Mass [kg] | Total [kg] | Mass [kg] | No | Mass [kg] | Total [kg] | Mass [kg] | No | Mass [kg] | Total [kg] |
| Electric Power | | | | 0.748 | | | | 0.2 | | | | 0.2 |
| Solar Cell | 0.18 | 1 | 0.18 | | 0 | 1 | 0 | | 0 | 1 | 0 | |
| Battery | 0.039 | 12 | 0.468 | | 0 | 12 | 0 | | 0 | 12 | 0 | |
| Power Controller | 0.1 | 1 | 0.1 | | 0.2 | 1 | 0.2 | | 0.2 | 1 | 0.2 | |
| Communication | | | | 1 | | | | 1.95 | | | | 8.1 |
| Receiver (L-band) | 0.2 | 1 | 0.2 | | 0.5 | 1 | 0.5 | | 0.5 | 1 | 0.5 | |
| Transmitter (S-band) | 0.5 | 1 | 0.5 | | 1 | 1 | 1 | | 3.4 | 1 | 3.4 | |
| Patch Antenna (S-band) | 0.1 | 2 | 0.2 | | 0 | 2 | 0 | | 0 | 2 | 0 | |
| Duplex Transceiver (VHF) | 0.05 | 1 | 0.05 | | 0.1 | 1 | 0.1 | | 3.1 | 1 | 3.1 | |
| Transmitter (UHF) | 0.05 | 1 | 0.05 | | 0.35 | 1 | 0.35 | | 1.1 | 1 | 1.1 | |
| Antenna (L, VHF, UHF) | 0 | 3 | 0 | | 0 | 3 | 0 | | 0 | 3 | 0 | |
| Attitude Determination and Control | | | | 1.04 | | | | 2.15 | | | | 2.15 |
| Magnetic Torquer | 0.12 | 3 | 0.36 | | 0.15 | 3 | 0.45 | | 0.15 | 3 | 0.45 | |
| Magnetic Sensor (3 Axis) | 0.1 | 1 | 0.1 | | 0.3 | 1 | 0.3 | | 0.3 | 1 | 0.3 | |
| Coarse Sun Sensor | 0 | 8 | 0 | | 0 | 8 | 0 | | 0 | 8 | 0 | |
| Gyro Sensor (1 Axis) | 0.06 | 3 | 0.18 | | 0.4 | 3 | 1.2 | | 0.4 | 3 | 1.2 | |
| Earth Horizon Sensor | 0.2 | 2 | 0.4 | | 0.1 | 2 | 0.2 | | 0.1 | 2 | 0.2 | |
| Command and Data Handling | | | | 1.2 | | | | 7 | | | | 7 |
| System Controller | 1.2 | 1 | 1.2 | | 7 | 1 | 7 | | 7 | 1 | 7 | |
| Structure and Mechanism | | | | 2.47 | | | | 1 | | | | 1 |
| Structure (Honeycomb Panel) | 1.5 | 1 | 1.5 | | 0 | 1 | 0 | | 0 | 1 | 0 | |
| Paddle Deployment Mechanism | 0.05 | 2 | 0.1 | | 0 | 2 | 0 | | 0 | 2 | 0 | |
| Paddle Drive Mechanism | 0.35 | 2 | 0.7 | | 0.5 | 2 | 1 | | 0.5 | 2 | 1 | |
| Antenna Deployment Mechanism | 0.02 | 1 | 0.02 | | 0 | 1 | 0 | | 0 | 1 | 0 | |
| Separation Mechanism | 0.15 | 1 | 0.15 | | 0 | 1 | 0 | | 0 | 1 | 0 | |
| Propulsion | | | | 4.2 | | | | 0 | | | | 0 |
| Propellant | 1.8 | 1 | 1.8 | | 0 | 1 | 0 | | 0 | 1 | 0 | |
| Thruster | 0.3 | 4 | 1.2 | | 0 | 4 | 0 | | 0 | 4 | 0 | |
| Propellant Tank | 1.2 | 1 | 1.2 | | 0 | 1 | 0 | | 0 | 1 | 0 | |
| Mission (for RO) | | | | 3.64 | | | | 16 | | | | 22 |
| GPS Receiver (for RO) | 2.5 | 1 | 2.5 | | 16 | 1 | 16 | | 22 | 1 | 22 | |
| Antenna (for POD) | 0.14 | 1 | 0.14 | | 0 | 1 | 0 | | 0 | 1 | 0 | |
| Antenna (for RO) | 0.5 | 2 | 1 | | 0 | 1 | 0 | | 0 | 1 | 0 | |
| Mission (for Thermal Infrared) | | | | 2.44 | | | | 1.2 | | | | 3 |
| GPS Receiver | 0.3 | 1 | 0.3 | | 0.2 | 1 | 0.2 | | 0.5 | 1 | 0.5 | |
| Antenna (for POD) | 0.14 | 1 | 0.14 | | 0 | 1 | 0 | | 0 | 1 | 0 | |
| Thermal Infrared Sensor | 2 | 1 | 2 | | 1 | 1 | 1 | | 2.5 | 1 | 2.5 | |
| Margin (5%) (for RO) | | | | 0.7 | | | | 1.4 | | | | 2.0 |
| Margin (5%) (for Thermal) | | | | 0.7 | | | | 0.7 | | | | 1.1 |
| Total (RO) | | | | 15.0 | | | | 29.7 | | | | 42.5 |
| Total (Thermal) | | | | 13.8 | | | | 14.2 | | | | 22.5 |

Tab 3 Link Budgets

| | L band Uplink | S band Downlink | VHF band Uplink | UHF band Downlink | Inter-Satellite (VHF) |
|---|----------------|-----------------|-----------------|-------------------|-----------------------|
| Frequency [GHz] | 1.20 | 2.40 | 0.14 | 0.43 | 0.14 |
| EIRP [dBW] | 54.72 | 4.31 | 28.70 | -0.59 | 3.47 |
| Transmitter Power [W] | 40.00 | 3.40 | 10.00 | 1.10 | 3.00 |
| [dBW] | 16.02 | 5.31 | 10.00 | 0.41 | 4.77 |
| Transmit Antenna Gain [dBi] | 40.00 | 0.00 | 20.00 | 0.00 | 0.00 |
| Transmitter Line Loss [dB] | -1.00 | -1.00 | -1.00 | -1.00 | -1.00 |
| Transmit Antenna Pointing Loss [dB] | -0.30 | 0.00 | -0.30 | 0.00 | -0.30 |
| Space Loss [dB] | -159.28 | -165.30 | -140.87 | -150.37 | -144.60 |
| Atmosphere Absorption Loss [dB] | -0.30 | -0.30 | -0.30 | -0.30 | 0.00 |
| Polarization Loss [dB] | -3.00 | -3.00 | -3.00 | -3.00 | -1.25 |
| Rain Attenuation [dB] | -1.00 | -1.00 | -1.00 | -1.00 | 0.00 |
| Other Loss [dB] | 0.00 | 0.00 | 0.00 | 0.00 | 0.00 |
| G/T | -28.90 | 18.10 | -28.90 | -4.70 | -23.70 |
| Receive Antenna Gain [dBi] | 0.00 | 40.00 | 0.00 | 20.00 | 0.00 |
| Receiver Line Loss [dB] | -1.00 | -0.30 | -1.00 | -0.30 | -0.30 |
| Receive Antenna Pointing Loss [dB] | 0.00 | -0.30 | 0.00 | -1.00 | 0.00 |
| System Noise Temperature [dBK] | -27.90 | -21.30 | -27.90 | -23.40 | -23.40 |
| Carrier-to-Noise Density Ratio | 90.84 | 81.41 | 83.23 | 68.64 | 62.52 |
| Required Carrier-to-Noise Density Ratio | 56.82 | 77.00 | 56.82 | 56.82 | 56.82 |
| Required Eb/N0 [dB] | 10.00 | 10.00 | 10.00 | 10.00 | 10.00 |
| Implementation Loss [dB] | 3.00 | 3.00 | 3.00 | 3.00 | 3.00 |
| Data Rate [kbps] | 9.60 | 1000.00 | 9.60 | 9.60 | 9.60 |
| [dBHz] | 39.82 | 60.00 | 39.82 | 39.82 | 39.82 |
| Bit Error Eb/N0 [dB] | 4.00 | 4.00 | 4.00 | 4.00 | 4.00 |
| Margin [dB] | 34.01 | 4.41 | 26.41 | 11.82 | 5.70 |

References

[1]H. Azuma, H. Okubo, Nanosatellite for land-sea-and-air multi earth observation and Attentive Citizens on Space, Congress of Institute of Electronics, Information and Communication Engineers, 2010 (in Japanese).

[2] R. Ichikawa et al., Removal Effects of propagation delay in analyses of GEONET/PPP by KARAT (in Japanese).

[3]T. Hobiger, et al., Ray-traced troposphere slant delays for precise point positioning, Earth Planet Space.

[4]Y. Shoji et al., Development of assimilation system for radio occultation data with four dimensional variation method, Report for development of environmental monitoring technology with precise positioning (in Japanese).

[5]G.Wuebbena et al., PPP-RTK: Precise Point Positioning Using State-Space Representation in RTK Networks, ION GNSS 2005.

[6]Atsushi Gomi, What Japanese GNSS should be, G-spatial EXPO2010, 2010 (in Japanese).